Drivers of measles mortality: the historic fatality burden of famine in Bangladesh

A. S. Mahmud; N. Alam; C.J.E. Metcalf
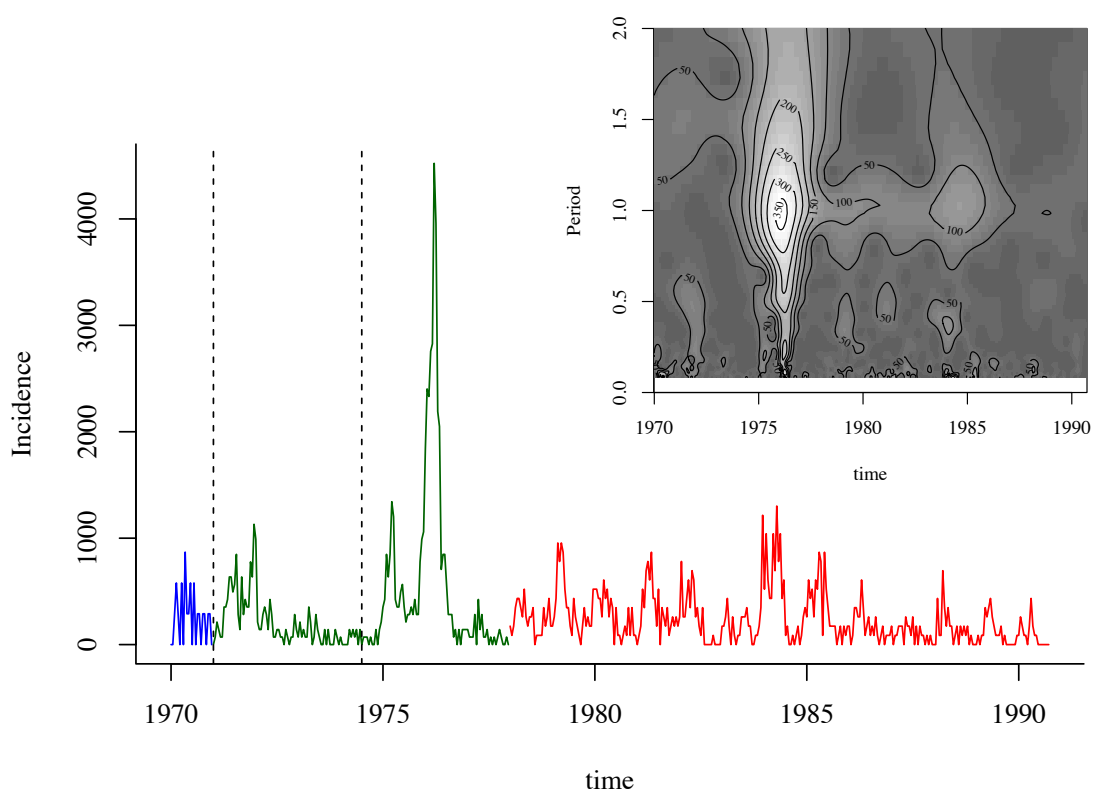
Supplementary Material

Fig. S1: Measles incidence in Matlab, Bangladesh, reconstructed from the deaths reports data using the estimated case-fatality rate (CFR). The three colors represent the three different data collection efforts over this time period (with varying numbers of villages under surveillance). The dashed vertical black lines indicate the onset of the war (1971) and the famine (1974). The inset figure shows the wavelet spectra for the reconstructed incidence. Lighter color indicates regions of higher power.
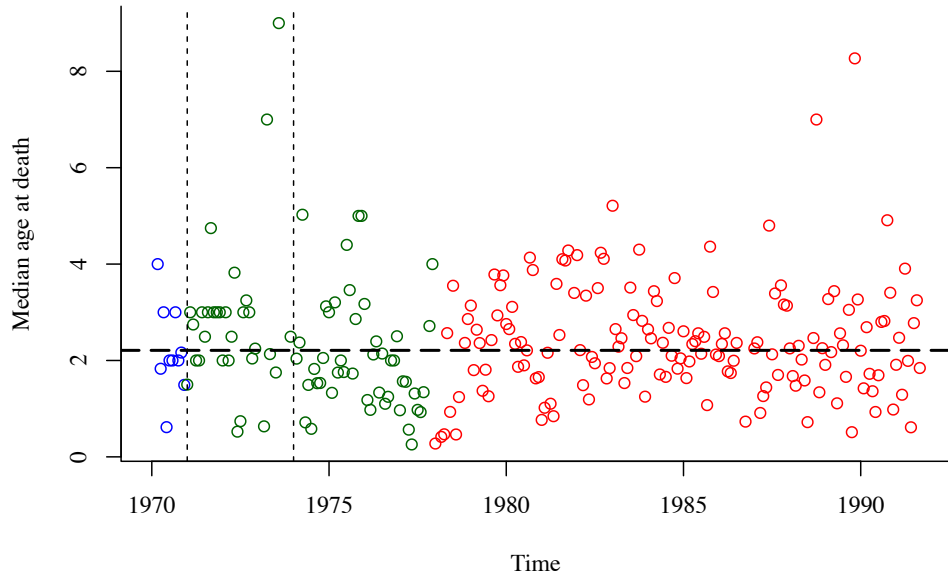
Fig. S2: Median age at death due to measles in Matlab. The median is computed for each month from January 1970 - September 1991. The three colors represent the three different data collection efforts over this time period. The dashed vertical black lines indicate the onset of the war (1971) and the famine (1974). The dashed horizontal black line indicates the median over the entire time period (2.22). The mean age at death was 2.85 over this period.
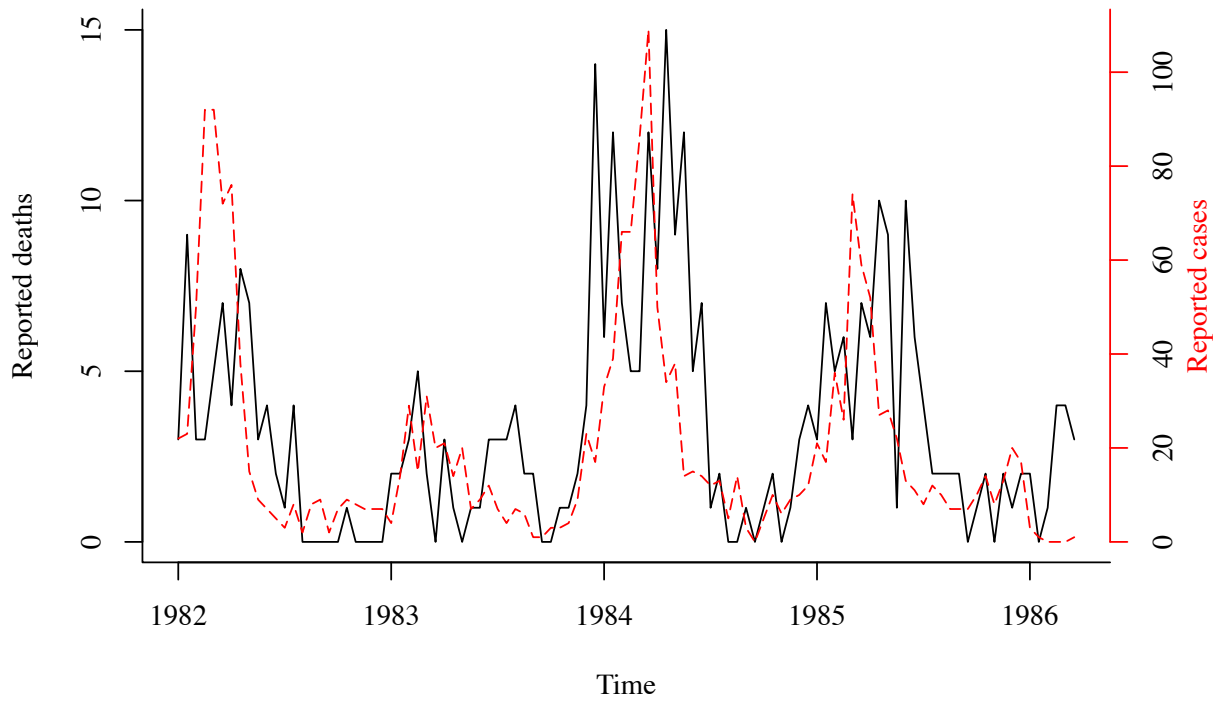
Fig. S3: Comparison of reported cases from a measles surveillance study in Matlab, and reported deaths due to measles. The surveillance was conducted between 1982 and 1985, and included 8135 vaccinated children between the ages of 9 and 60 months of age and a randomly matched group of non-vaccinated children.
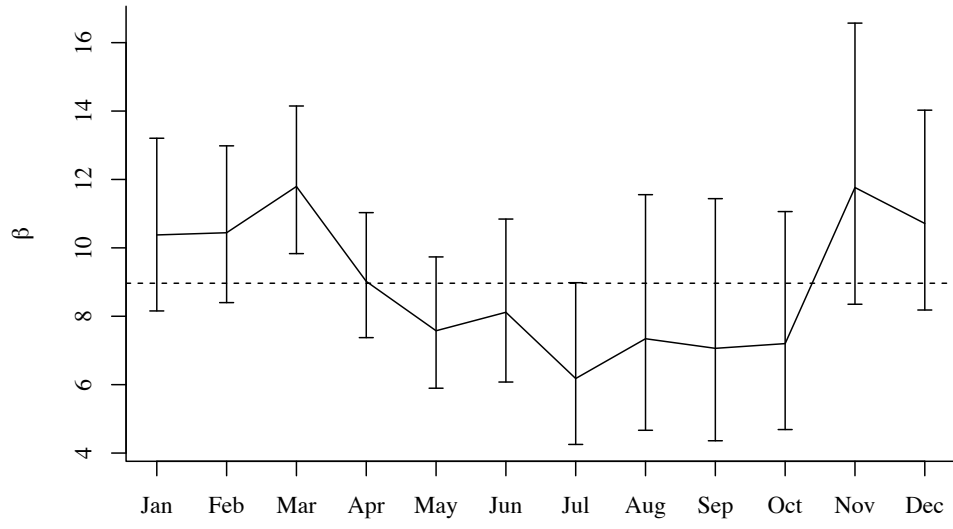
Fig. S4: Seasonal measles transmission rates, and 95% confidence intervals, in Matlab. Transmission rates were estimated using the time series Susceptible-Infected-Recovered model (TSIR) fit to mortality data.
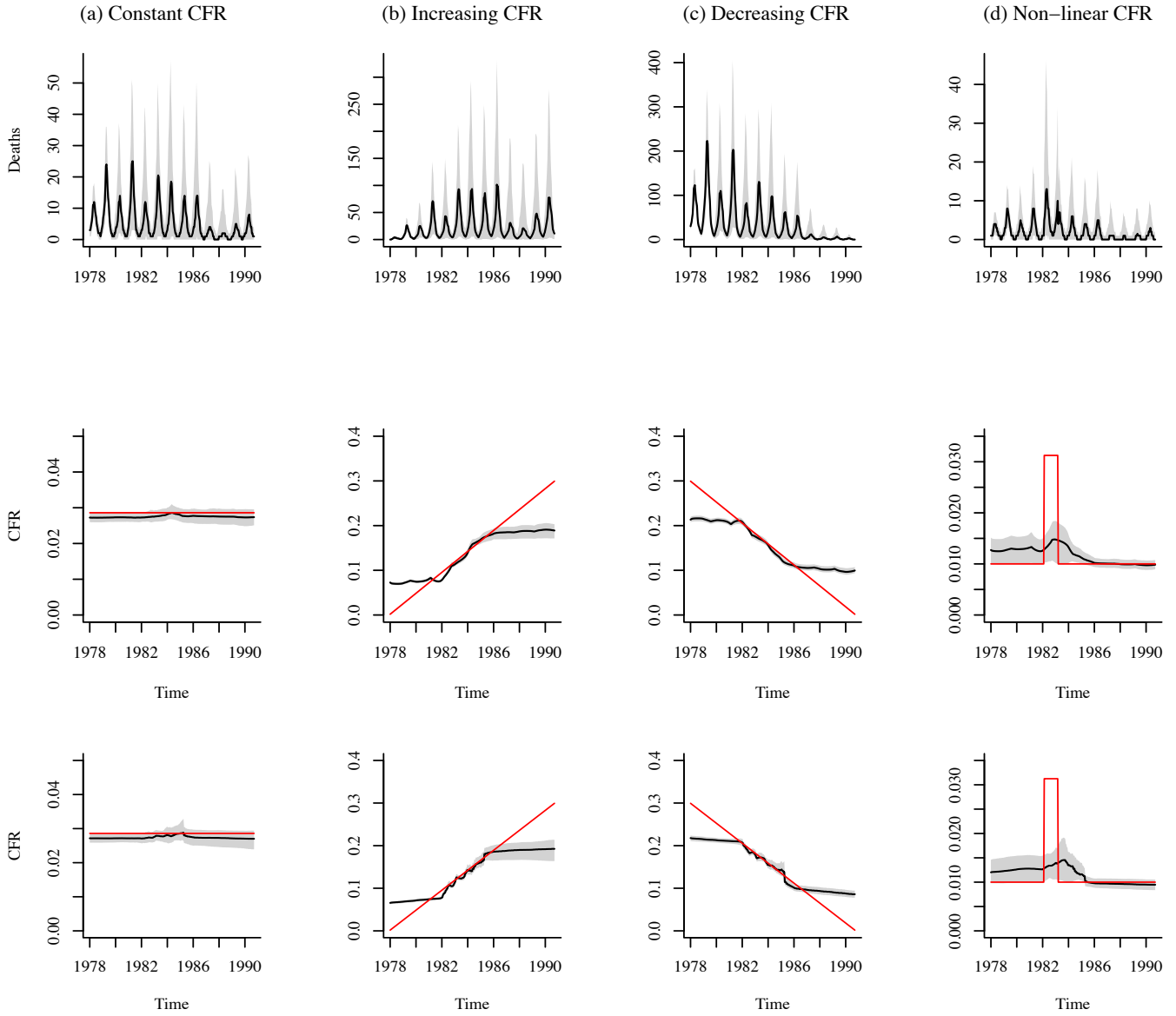
Fig. S5: Estimates of CFR using loess regression (middle panel) and lowess regression (bottom panel) of cumulative births on cumulative simulated deaths. Stochastic simulations of deaths are shown in the top panel of plots. Black line shows the median of 500 simulations; the shadowed region corresponds to the range between the 10th and 90th percentiles of the simulations. Deaths were simulated assuming four scenarios: (a) constant CFR = 0.02; (b) linearly increasing CFR over the time period, c) linearly decreasing CFR over the time period, and d) non-linear CFR with an increase in the middle of the time period. The bottom panel of plots shows median estimated CFR in black; the shadowed region corresponds to the range between the 10th and 90th percentiles of the estimates. Red line indicates the actual CFR assumed for each simulation scenario.
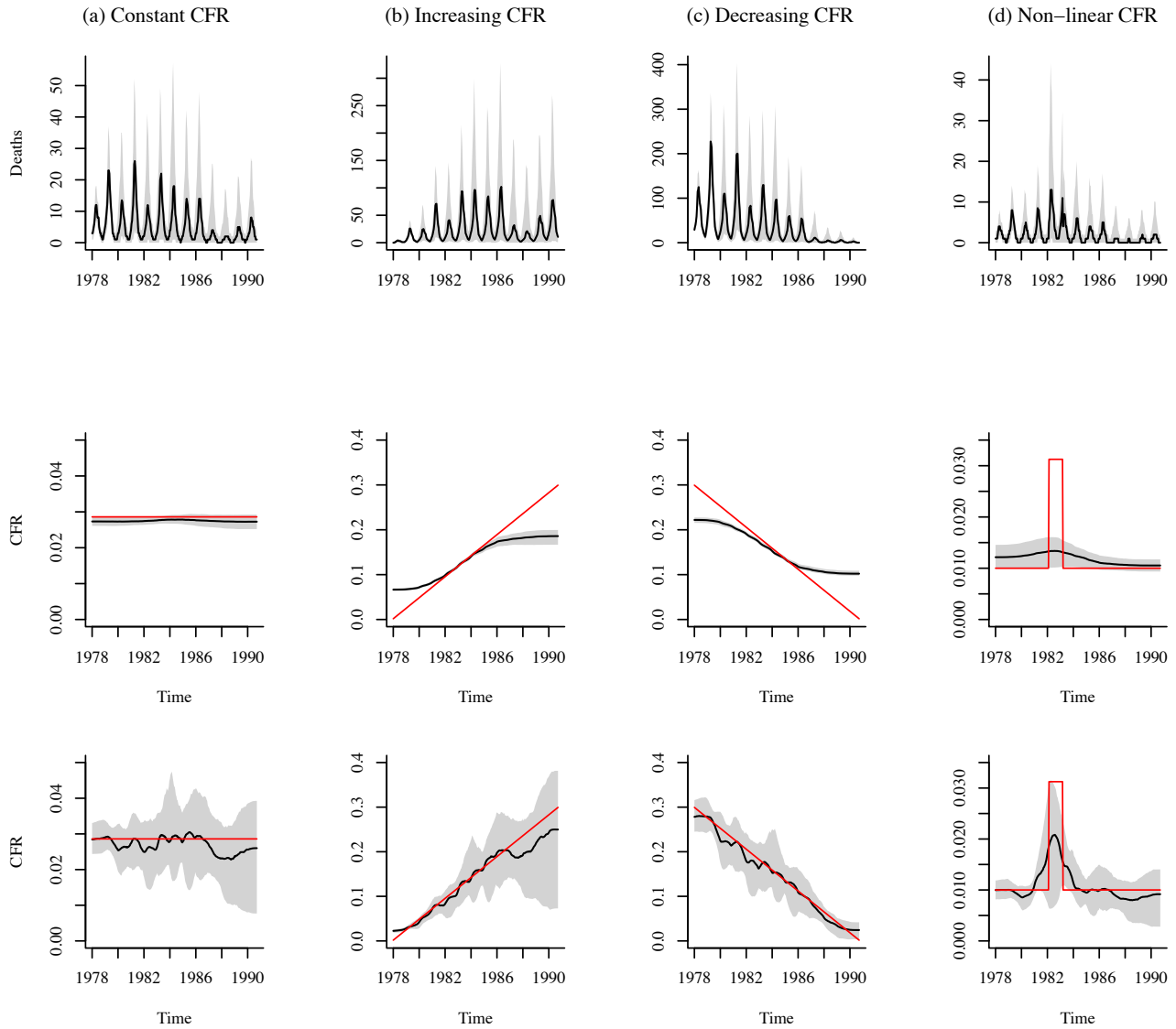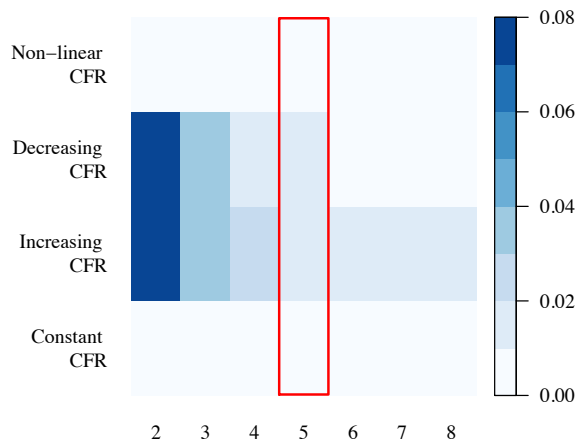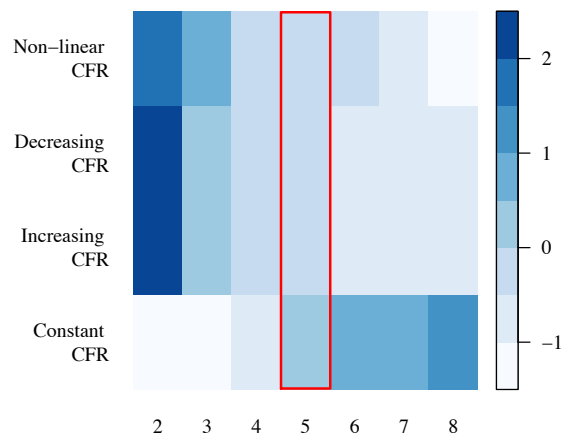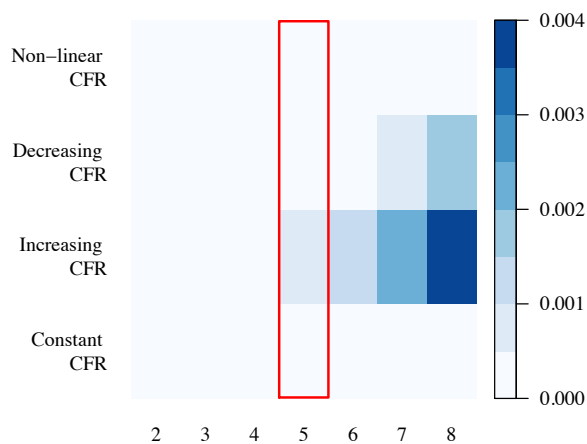
Fig. S6: Estimates of CFR using spline regression of cumulative births on cumulative simulated deaths. Stochastic simulations of deaths are shown in the top panel of plots. Black line shows the median of 500 simulations; the shadowed region corresponds to the range between the 10th and 90th percentiles of the simulations. Deaths were simulated assuming four scenarios: (a) constant CFR = 0.02; (b) linearly increasing CFR over the time period, c) linearly decreasing CFR over the time period, and d) non-linear CFR with an increase in the middle of the time period. The bottom two panel of plots shows median estimated CFR in black; the shadowed region corresponds to the range between the 10th and 90th percentiles of the estimates. Red line indicates the actual CFR assumed for each simulation scenario. The middle panel shows the results of using spline regression with 3 degrees of freedom; the bottom panel shows the results of using spline regression with 8 degrees of freedom.
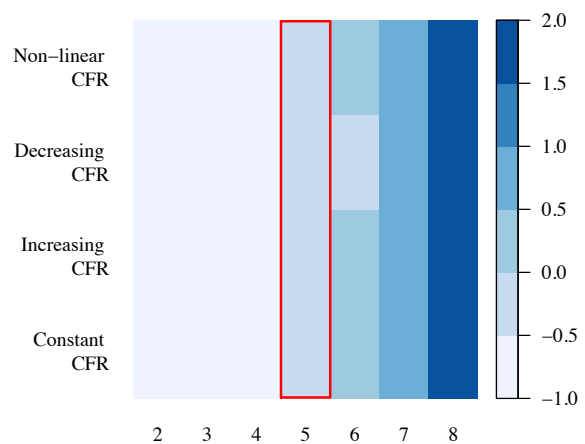
(a) Mean absolute error

(b) Scaled mean absolute error

(c) Mean variance

(d) Scaled mean variance

Fig. S7: Comparison of mean absolute error and mean variance (means over the entire time series) of CFR estimated using spline regressions with degrees of freedom ranging from 2 to 8 (x-axis for each plot) for each simulation scenario (y-axis for each plot). Figures S7b and S7d show the error and variance scaled within each simulation scenario. Absolute error and variance were largest for the linearly increasing and decreasing CFR scenarios. Spline regressions with larger degrees of freedom generally had lower error since they were better able to capture the temporal trend in CFR, but tended to overfit to the mortality time series resulting in larger variance. For our main results, we use spline regression with 5 degrees of freedom (highlighted in red).
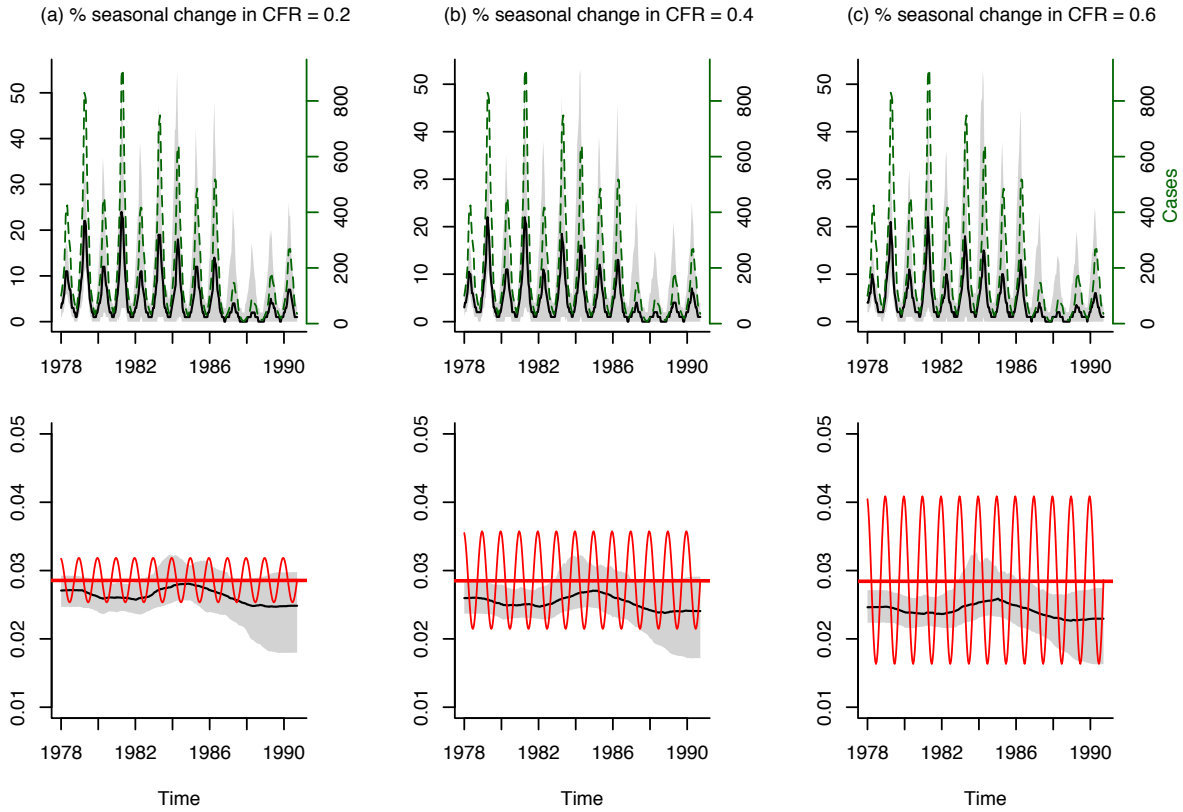
Fig. S8: Estimates of seasonally-varying CFR using spline regression (with 5 degrees of freedom) of cumulative births on cumulative simulated deaths. Stochastic simulations of deaths (black) and cases (dashed green) are shown in the top panel of plots. Black and green lines show the median of 500 stochastic simulations; the shadowed region corresponds to the range between the 10th and 90th percentiles of the simulated number of deaths. Deaths were simulated assuming three seasonally-varying CFR scenarios represented by sine functions with different amplitudes and same mean. The bottom panel of plots shows median estimated CFR in black; the shadowed region corresponds to the range between the 10th and 90th percentiles of the estimates. Red line indicates the actual CFR assumed for each simulation scenario.
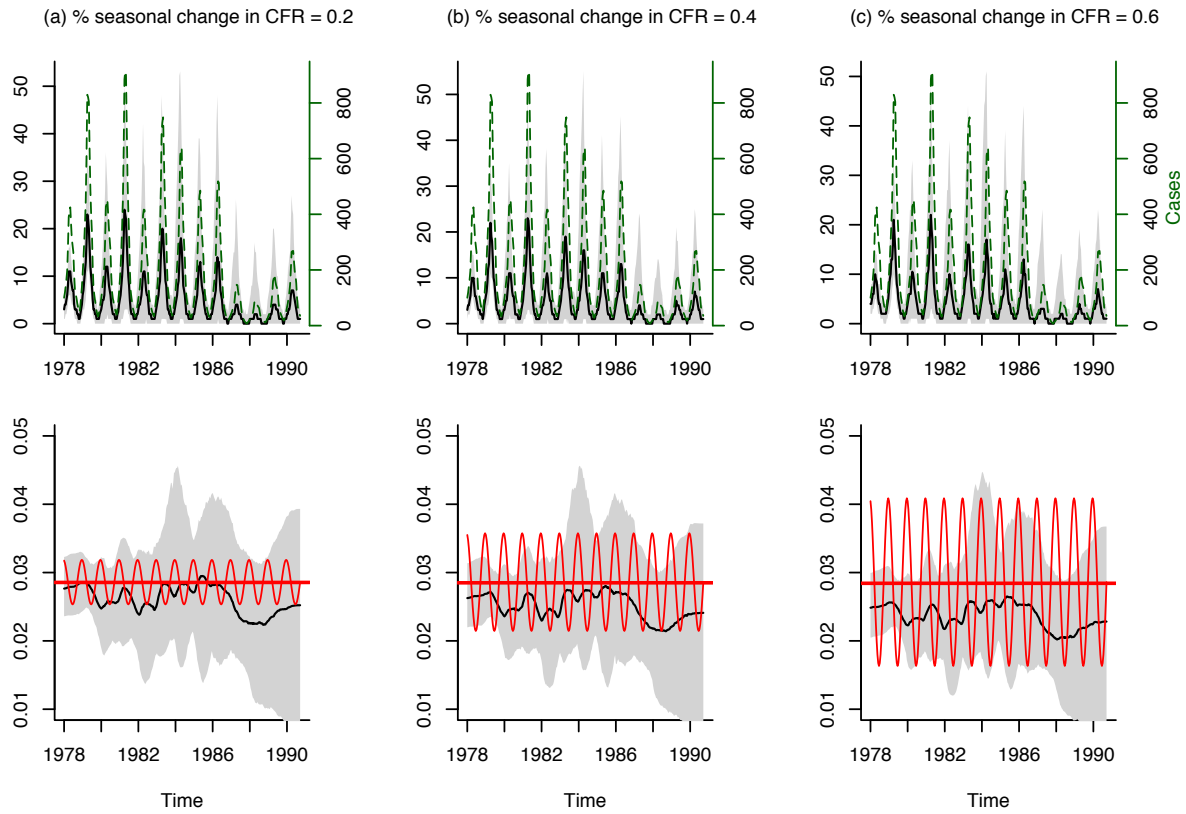
Fig. S9: Estimates of seasonally-varying CFR using spline regression (with 8 degrees of freedom) of cumulative births on cumulative simulated deaths. Stochastic simulations of deaths (black) and cases (dashed green) are shown in the top panel of plots. Black and green lines show the median of 500 stochastic simulations; the shadowed region corresponds to the range between the 10th and 90th percentiles of the simulated number of deaths. Deaths were simulated assuming three seasonally-varying CFR scenarios represented by sine functions with different amplitudes and same mean. The bottom panel of plots shows median estimated CFR in black; the shadowed region corresponds to the range between the 10th and 90th percentiles of the estimates. Red line indicates the actual CFR assumed for each simulation scenario.
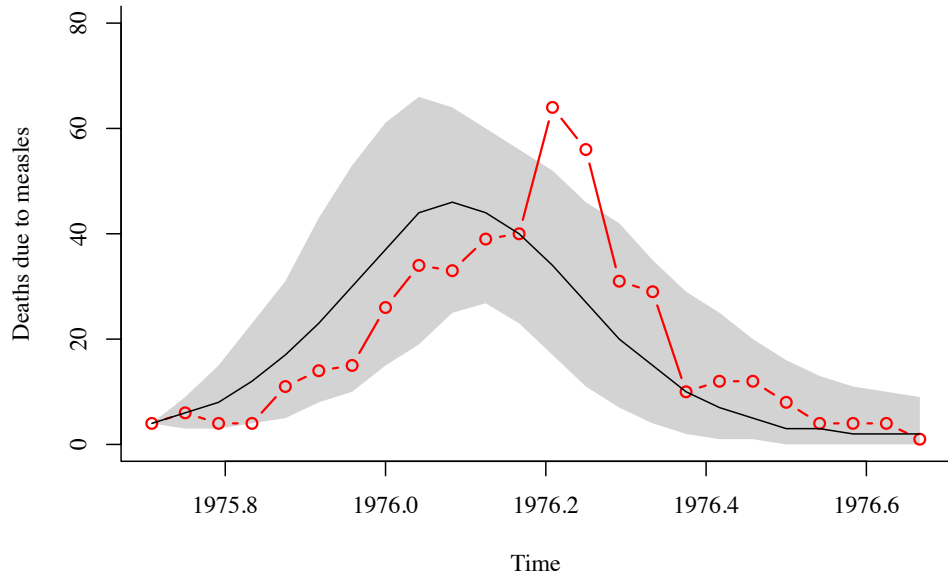
Fig. S10: Reported deaths from measles between October, 1975 and July, 1976 (in red). Black line shows the median of 1000 stochastic simulations of the chain-binomial model; the shadowed region corresponds to the range between the 10th and 90th percentiles of the simulations. Our fitted model consistently peaks earlier than the observed number of deaths; however, we are able to capture both the decline of the outbreak and the total size of the outbreak.

Fig. S11: Histogram showing the birth date distribution for those who died from measles during the 1976 outbreak. The red bar indicates the number of children who were born during the 1974 famine and died during the 1976 measles outbreak.
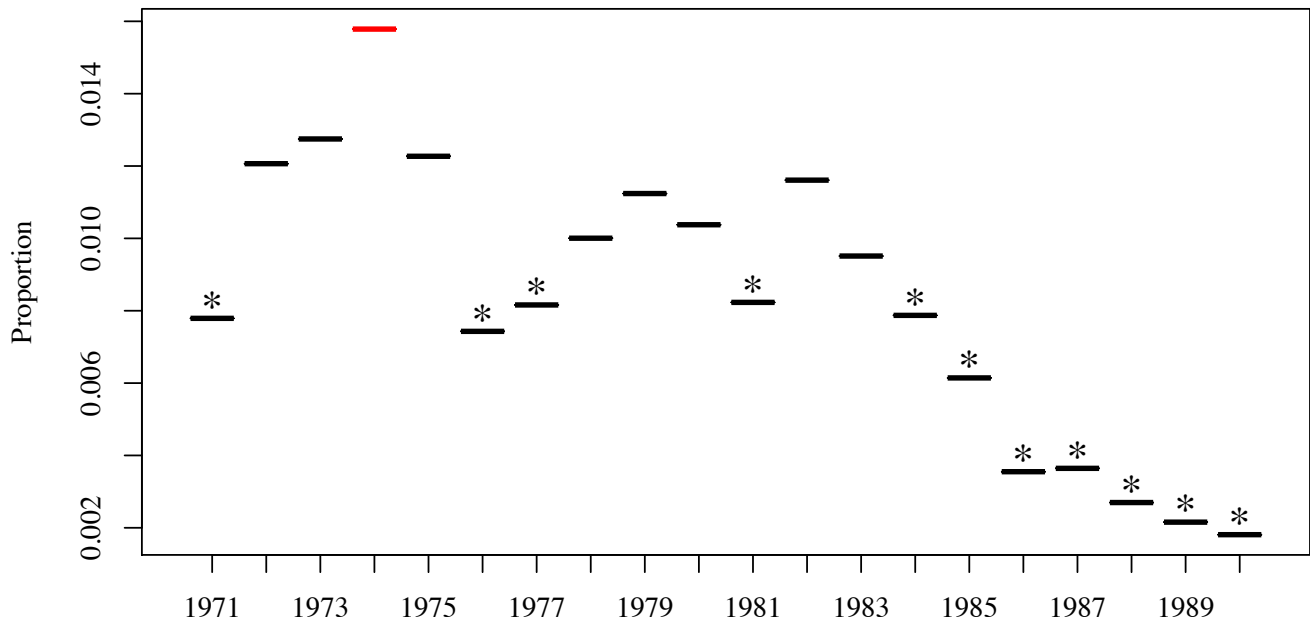
Fig. S12: Proportion of children born each year who die from measles within three years of birth. ∗ signifies that the proportion is significantly different from the 1974 (famine year) proportion (shown in red) at the 95% level, after correcting for multiple testing. The proportion is much lower from 1985 onwards due to the introduction of vaccination.